Initial insights into releasing bound biomarkers from kerogen matrices using microscale sealed vessel catalytic hydrogenation (MSSV-HY)

Liangliang Wu[a*], Brian Horsfield[b]

[a]*State Key Laboratory of Organic Geochemistry, Guangzhou Institute of Geochemistry, Chinese Academy of Sciences, Wushan, Guangzhou 510640, P.R. China*

[b]*GFZ German Research Centre for Geosciences, Potsdam 14473, Germany*

[*] Corresponding author: Tel: +86 20 87597391; Fax: +86 20 87597391; E-mail address: wuliangliang@gig.ac.cn (L. Wu)

ABSTRACT

Microscale Sealed Vessel pyrolysis (MSSV) is a microanalytical technique originally developed for artificially maturing sedimentary organic matter and examining the bulk compositional relationships between kerogen and petroleum. Here, we explore the possibility of modifying the standard MSSV pyrolysis approach to increase biomarker release from macromolecular matrices. This is termed microscale sealed vessel catalytic hydrogenation, or MSSV-HY. Tetralin is employed as hydrogen donor and dispersed sulfide molybdenum as catalyst. Using two kerogen concentrates, one of low maturity (vitrinite reflectance: 0.6 %Ro) and the other over-mature (1.8 %Ro), from the Dalong Mudstone (Permian, Sichuan Basin), the effects of tetralin and catalyst alone and as mixtures, and the tetralin/kerogen ratio on biomarker release have been investigated, and optimum conditions identified. A comparison of results with those of HyPy enabled the utility of the method to be assessed. Biomarkers were generated from the over-mature sample and preserved using MSSV-HY, whereas they were absent in MSSV products. Biomarkers released from the low maturity sample using MSSV were devoid of extended hopanes, and dominated by C_{27} steranes, whereas the MSSV-HY products were rich in Tm, the extended hopanes, and with C_{27}–C_{29} regular steranes. MSSV-HY products showed some similarities to HyPy products. The steranes from MSSV-HY were very similar to those from HyPy; although some differences in hopane distributions were discernable (e.g., the abundances of Ts and C_{30} hopane) due to varied contribution of occluded OM in the HyPy and MSSV-HY analyses. This proof of concept study has shown that off-line

MSSV-HY shows great promise as a means for releasing bound biomarkers and reducing secondary cracking because of catalyst associated pressure increase in the MSSV tubes. Its currently planned area of operation is in petroleum systems.

Keywords: bound biomarkers, microscale sealed vessel pyrolysis, catalytic hydrogenation, MSSV, MSSV-HY, Sichuan Basin, Dalong Formation

1. Introduction

Microscale Sealed Vessel pyrolysis is a microanalytical technique originally developed for artificially maturing sedimentary organic matter and then quantifying GC-amenable products (C_{1+}) in a single analytical step (Horsfield et al., 1989; 2015). The main operational advantage of MSSV pyrolysis is its high precision and reproducibility, milligram sample loading capacity, and batch processing capability. It is well suited to examining the bulk compositional relationships between kerogens, asphaltenes and petroleum. Thus, bulk petroleum characteristics (gas-oil ratio, PVT behaviour), as well as fluid stabilities (oil-to-gas cracking) and generation parameters (primary cracking kinetics), have been predicted for lacustrine and marine systems using MSSV pyrolysis and, crucially, the results verified by comparison with natural petroleum systems (e.g., Horsfield et al., 1992; Schenk et al., 1997; Dieckmann et al., 1998; di Primio and Horsfield, 2006; Keym et al., 2006; Lehne et al., 2009; Yang and Horsfield, 2016). All of these protocols were based on pyrolysis products which occur in high yield such as *n*-alkanes and aromatic hydrocarbons.

Biomarkers are incorporated into kerogen, asphaltenes and humic substances by covalent bonding (Mycke et al., 1987; de Leeuw et al., 1989; Hoffman et al., 1992; Richnow et al., 1992; Adam et al., 1993) as well as by adsorption and absorption (Snowdon et al., 2016; Cheng et al., 2016). A variety of pyrolysis configurations, incorporating open and closed systems, variable pressure constraints and under broadly hydrous or anhydrous conditions, have been used to release and analyse bound biomarkers for tracking the evolution of life, assessing paleoenvironments, conducting pollution studies, and performing oil-oil and oil-source correlations (e.g., Gallegos, 1975; Seifert, 1978; Seifert and Moldowan 1980; Eglinton and Douglas 1988; Comet et al., 1986; Love et al., 1995; Lewan, 1997; Koopmans et al., 1998; Greenwood et al., 2006; Berwick et al., 2007, 2011). In most of these pyrolysis systems the original stereochemistry of bound biomarkers is not well preserved. The exception to this is catalytic hydropyrolysis (HyPy), which utilises a dispersed sulphided molybdenum catalyst and high hydrogen pressures (>10 MPa) to ensure minimal structural rearrangement of the released biomarkers (Love et al., 1995, 1996, 1997; Murray et al., 1998, Meredith et al., 2008). Due to the protection afforded by their macromolecular hosts, the thermal maturity of bound biomarkers is lower than that of their freely occurring counterparts (Rubinstein et al., 1979; Behar et al., 1984; Russell et al., 2004; Lockhart et al., 2008; Wu et al., 2013). Of direct relevance to the present study, Berwick et al. (2010) made a detailed comparison of MSSV pyrolysis (Quantum MSSV-1 Thermal Analysis System®) with HyPy, and documented a great many product similarities, as well as allocating important advantages to each

technique. As far as the retention of biomarker stereochemistry was concerned, it was concluded that HyPy displays less secondary alteration than does MSSV, reflecting more selective bond cleavage.

Here, we explore the possibility of modifying the standard MSSV pyrolysis approach in order that the stereochemistry of biomarkers released from macromolecular matrices is preserved better. From our perspective, such a development would allow both paleoenvironment to be assessed and compositional kinetic models to be built using the same pyrolysis system. Termed MSSV catalytic hydrogenation (MSSV-HY), the new method uses tetralin as hydrogen donor and employs a dispersed sulphidic molybdenum catalyst. Tetralin was chosen as hydrogen donor because it has been widely used as such in coal liquefaction (Vlieger, 1988 and References therein). The capacity of the hybrid MSSV-HY approach to improve structural preservation of biomarkers released from kerogen during MSSV experiments was here assessed by comparison to the biomarker products released by traditional HyPy analysis of the same sample suite.

2. Samples and methods

Wu et al. (2013) used HyPy with ammonium dioxydithiomolybdate [$(NH_4)_2MoO_2S_2$] to release and analyse bound biomarkers from mudstones of the Dalong Formation (Permian), Sichuan Basin, China. Two samples from that series were used in the tests described here, namely one of low maturity (GY-8: vitrinite reflectance: 0.6 %Ro) and the other of high maturity (WC-4A: 1.8 %Ro). The same

catalyst used by Wu et al. (2013) was also used. Test experiments were carried out and the pyrolysis products qualitatively and quantitatively analyzed by thermovaporization-gas chromatography (Tvap-GC) and off-line GC–MS in order to optimize the conditions required for releasing biomarkers using MSSV-HY.

2.1. Sample preparation

The Dalong Formation mudstone sample of GY-8 (collected at latitude 32°19′11″N, longitude 105°27′18″E) has a total organic carbon content (TOC) of 8.76%, a Hydrogen Index (HI) of 343 mgHC/gTOC, an atomic H/C of 0.87 and is of low maturity (0.6 %Ro; T_{max} = 438 °C). The kerogen concentrate prepared from this sample has a weight percent carbon of 67.6 and is classed as Type II (-III). The Dalong Formation mudstone sample WC-4A (collected at latitude 32°18′45″N, longitude 106°16′26″E) has a TOC of 2.81% and a HI of 5 mgHC/gTOC. It is an over-mature Type II (-III) kerogen (1.8 %Ro; T_{max} = 603 °C) (Wu et al., 2012, 2013). The WC-4A kerogen concentrate prepared from this sample has carbon content of 79.7 wt%.

Each source rock sample was crushed to < 80 mesh. Then, sample powders were Soxhlet extracted using a mixture of DCM and MeOH (93:7, v/v) to supply the free bitumen from which biomarkers were analysed and compared with those from pyrolysis. Kerogen isolation from minerals was performed using acid treatment. Carbonates were removed using 1 N HCl (80 °C for 4 h) followed by washing of the residue using distilled water and employing centrifugation. A mixture of HCl and HF

was then used to remove silicates (80 °C for 4 h), and the solid residue recovered by water washing and centrifugation. Both steps were repeated. The isolated kerogen concentrate was then extracted with an ternary solvent azeotrope (benzene/acetone/methanol: 5:5:2, v/v/v) using Accelerated Solvent Extraction (ASE) to remove bitumen-2, which is intimately associated with the kerogen (Wilhelms et al., 1991).

2.2. MSSV and MSSV-HY pyrolysis experiments

MSSV pyrolysis was conducted on the two kerogen concentrates. About 5 mg of each kerogen concentrate was weighed into a glass capillary that had been sealed at one end, then the internal volume of the tube was reduced from ca. 40 µl to ca. 15 µl using pre-cleaned quartz sand. The tube was then sealed shut using a H_2 flame.

For catalyst-assisted MSSV-HY experiments the solvent-extracted kerogen was impregnated with an aqueous solution of ammonium dioxydithiomolybdate [$(NH_4)_2MoO_2S_2$] to give a nominal loading of 5 wt% molybdenum. Then, aliquots of about 3 mg of the pretreated kerogen powder, together with tetralin were sealed in glass capillaries for MSSV pyrolysis. Different ratios of tetralin/ kerogen (T/K ratio shown in Table 1) were used to investigate the influence of tetralin on the released biomarkers in MSSV-HY. Additionally, MSSV pyrolysis of: (i) kerogen with tetralin; and (ii) kerogen with catalyst were conducted to investigate the respective role of tetralin and catalyst on kerogen pyrolysis. It should be noted that $(NH_4)_2MoO_2S_2$ is

not the catalyst but it decomposes to form the active catalyst molybdenum disulfide (MoS_2) within the MSSV tube at pyrolysis temperatures above 250 °C in the presence of H_2 (Zelenski and Dorhout, 1998; Boone and Ekerdt, 2000). MoS_2 is used as a catalyst in many processes, including hydrodesulphurization and CO methanation reactions (Bevanente et al., 2002; Farag et al., 2009; Shi et al., 2009).

Pyrolysis was performed using an external high performance oven consisting of a cartridge-heated massive cylindrical metal block acting as a circular sample holder which provided a very homogeneous temperature field throughout the core. Previous studies have concluded that C–C bond scission begins to occur to a significant extent when the temperature is higher than 400 °C (e.g., Brown et al., 1994; Love et al., 1995). After several test experiments, 400 °C and 120 min were chosen for both MSSV and MSSV-HY pyrolysis experiments in this study. Under these conditions the yields of *n*-alkanes and hopanes reach their respective maximum value, reflecting a balance between the release and subsequent cracking of bound biomarkers (Fig. 1).

Two aliquots sealed in glass capillaries were pyrolysed for each set of experimental conditions, one for on-line thermovaporisation (Tvap)-gas chromatography analysis using the Quantum MSSV-2 Thermal Analysis System ®, and the other for off-line analysis using GC–MS. Prior to Tvap analysis, the outer surface of each primed capillary was purged at 300 °C for 5 min to remove contaminants. The capillary was then crushed by a piston device, thus releasing volatilisable pyrolysis products to a liquid nitrogen cooled trap (–178 °C). After 10

167 min, products were liberated (300 °C) and directly transferred into an Agilent GC
168 6890A gas chromatograph, the details of which are described by Keym et al. (2006).
169 An HP-Ultra l (50 m × 32 mm i.d.) dimethylpolysiloxane-coated column and flame
170 ionization detector (FID) was used. *n*-Butane was used as an external standard to
171 quantify the individual compounds.

172 The second capillary was cracked open off-line, and the non-gaseous
173 pyrolysate extracted using dichloromethane and methanol (90:10, v:v). Heating in a
174 sand bath at 50 °C for 60 min removed excess solvent, unspent tetralin and aromatic
175 reaction products (mainly naphthalene) in the C_6–C_{12} range. Asphaltenes were
176 precipitated from the above products by adding 50:1 (v/v) cold *n*-hexane, followed by
177 centrifugation. The maltene fractions were then separated by medium pressure liquid
178 chromatography (MPLC) into saturated, aromatic and polar fractions, using the
179 procedure reported by Radke et al. (1980). The MPLC was equipped with a thermally
180 deactivated silica 100 pre-column and a LiChroPrep Si60 main column and run with
181 *n*-hexane as mobile phase. The saturated biomarkers were analyzed using a Thermo
182 Scientific Trace GC Ultra gas chromatograph coupled to a DSQ mass spectrometer. A
183 fused silica capillary column (SGE BPX5, 50 m length, 0.22 mm i.d. × 0.25 μm film
184 thickness) was used. The GC oven was held isothermally at 50 °C for 1 min,
185 programmed to 310 °C at 3 °C/min rate, with a final hold time of 30 min. Helium was
186 used as carrier gas with a constant flow rate of 1.5 mL/min. The injector temperature
187 was programmed from 50 °C to 300 °C at a rate of 10 °C/s and held there for 10 min.
188 The source temperature was 260 °C. The ion source was operated in the electron

impact (EI) mode with electron energy of 70 eV. 5α-Androstane was used as an internal standard for the quantification of the saturated hydrocarbon fraction. The same fractionation and analytical approach was employed to characterize free biomarkers whose compositions were then compared with pyrolysates in the course of the study.

3. Results and discussion

3.1. MSSV-HY optimization experiments

3.1.1. Liquid hydrocarbon yield

MSSV-HY optimization experiments were performed on the low maturity kerogen concentrate GY-8. The gas chromatographic fingerprints of the on-line thermovaporised C_{1+} pyrolysis products from kerogen alone and mixed with tetralin are given in Fig. 2. *n*-Alkane homologues are readily recognizable in the gas chromatogram, ranging up to C_{33}. Naphthalene is the dominant compound, and unspent tetralin is present. Binaphthalenes are also generated in the pyrolysis products of kerogen and tetralin together, from the dimerization reaction which is catalyzed by both clay minerals and pyrite (Sundaram et al., 1983). While this makes the aromatic fraction unusable for further analysis, biomarkers in the saturated fraction released by MSSV-HY remain unaffected.

The yields of total solvent extractables, saturate and aromatic fractions, as well as total *n*-alkanes and total hopanes in the products of MSSV and MSSV-HY experiments are shown in Table 1. The total conversion of kerogen to liquid products

(C_{15+}) for the MSSV pyrolysis of kerogen alone is 38%, and 39% when catalyst is present. This climbs to 41% when tetralin is used. Importantly, the catalytic effect is more pronounced when both catalyst and tetralin are used, with the apparent total conversion of kerogen to liquid products (C_{15+}) over 100% being caused by contributions from tetralin pyrolysis products (such as binaphthalenes for some experiments).

3.1.2. The role of catalyst and tetralin

Fig. 3 shows the distribution of steranes and hopanes resulting from the MSSV experiments on kerogen alone (MSSV-1), kerogen with catalyst (MSSV-2), kerogen with tetralin (MSSV-3), and kerogen with catalyst and tetralin together (MSSV-HY). C_{29} 17α(H),21β(H)-hopane (H29) is the biggest *m*/*z* 191 peak in all MSSV experiments, while C_{30} 17α(H),21β(H)-hopane (H30) is the biggest *m*/*z* 191 peak in MSSV-HY products. Extended hopanes up to C_{33} are detected in MSSV-1 and MSSV-2 products, whereas the range extends up to C_{35} for the MSSV-3 (tetralin) and MSSV-HY (tetralin + catalyst) products. The distributions of C_{27}–C_{29} ααα*R* steranes in the MSSV-HY products exhibit a $C_{27} \approx C_{29} > C_{28}$ fingerprint, while all MSSV products exhibit a C_{27} predominance ($C_{27} > C_{29} > C_{28}$) (Fig. 3). These results demonstrate that both the catalyst and tetralin (H-donor) are required to enhance the release of bound biomarkers.

As alluded to earlier, $(NH_4)_2MoO_2S_2$ decomposes during pyrolysis to active MoS_2 (Zelenski and Dorhout, 1998; Boone and Ekerdt, 2000). The active MoS_2 can

be further reduced to Mo and H_2S by H_2 at high temperature (He et al., 2011). Meanwhile, increasing H_2S/H_2 will promote the catalytic activity of MoS_2 (Farag et al., 2009). Farag et al. (2009) suggested that the catalytic mechanism of MoS_2 was: first, free radical reactions initiated by H_2S derived from decomposition of catalyst precursor and reduction of active MoS_2; and then the dissociation of H radicals at the Lewis acid site of Mo. Thus, initiation of the full catalytic effect of MoS_2 requires a sufficient supply of H_2.

Tetralin plays two roles in MSSV-HY. Firstly, it acts as a hydrogen donor (the same role as hydrogen gas in HyPy) to quench radical pyrolysates, and secondly, tetralin also suppresses the cross-linking reactions of kerogen fragments due to the penetration of tetralin into the micropores (Lewan, 1997). Gates (1979) suggested that tetralin plays the role of hydrogen carrier in the coal liquefaction process, with the catalyst promoting hydrogen addition reactions. That is, tetralin gives up hydrogen to the pyrolysis fragments, and then returns to the catalyst surface, where it reacts with adsorbed hydrogen and is converted into tetralin again (Gates, 1979). Pyrolysis reaction pathways can be simply described by a free-radical mechanism where competing thermal cracking and cross-linking reactions occur (Lewan, 1997). The generated free radicals need to be stabilized by a hydrogen donor to form stable components, or else they will undergo further radical propagation reactions.

3.1.3. Effect of the tetralin/kerogen ratio

Fig. 4 shows the patterns of hopanes and steranes released by MSSV-HY at

various tetralin/kerogen (T/K) ratios. With increasing T/K ratio, the patterns of hopanes released by MSSV-HY remain quite stable, whereas there are some differences among the distributions of released steranes. Hopanes are thermally more stable than steranes (e.g, Wu et al., 2016). The work by Michels et al. (1994) also reported that pressure has no significant influence on hopane profiles, while sterane profiles seems to be changed when a different pressure was used.

Fig. 5 shows the evolution trend of (S21+S22)/(C_{27}+C_{28}+C_{29}) regular steranes ratio with increasing T/K ratio. As the tetralin/kerogen ratio increases from 0 to 5, the ratio of (S21+S22)/(C_{27}+C_{28}+C_{29}) regular steranes is reduced from 0.72 to 0.23 (Table 2, Fig. 4), the latter value approaching that of 0.13 measured using HyPy experiments (Table 3). In this regard, it is noteworthy that diginane (S21: 5α,14β,17β(H)-pregnane) and 20-methyldiginane (S22: 5α,14β,17β(H)-homopregnane) are the more thermodynamically stable forms of pregnane and 20-methylpregnane (Wingert and Pomerantz, 1986). Previous researchers have pointed out that pregnane and homopregnane may originate from the thermal cracking of C_{27}–C_{29} regular steroids (Huang et al., 1994; Abbott et al., 1995). The recent work by Wang et al. (2015) further suggested that 5α,14β,17β(H)-pregnane, 5α,14β,17β(H)-homopregnane and higher C_{23}–C_{26} 20-*n*-alkylpregnanes are products from the cracking of steroids bound to the kerogen. This means that the ratio of (S21+S22/(C_{27}+C_{28}+C_{29}) regular steranes could be reflecting the degree of cracking within the pyrolysis system: the more tetralin present the less severe is the cracking of covalently bound steranes.

The distributions of C_{27}–C_{29} regular steranes in products of MSSV-HY also

changes with an increase in the T/K ratio, with the relative abundance of C_{29} regular steranes gradually increasing (Fig. 6). When the T/K ratio is < 2:1 the distribution of C_{27}–C_{29} regular steranes released by MSSV-HY exhibits a C_{27} predominance (C_{27} > C_{29} > C_{28}). However, when the T/K ratio is raised to 5 the MSSV-HY products exhibit a similar $C_{27} \approx C_{29} > C_{28}$ distribution, corresponding to a decreased influence of secondary cracking.

Since the amount of kerogen used in each MSSV-HY experiment is essentially constant, the presence of higher T/K ratios corresponds to higher partial pressures and higher relative abundances of H-donors in the reaction system. With regard to pressure, Hamann et al. (1963) pointed out that free radical and molecular dissociation is retarded by a high partial pressure of reactants. Pyrolysis experiments on the light aromatic fraction of a crude oil at 375 °C under various pressures showed that secondary cracking of the C_{15} C_{20} and C_{20+} compounds were reduced when the pressure was increased from 100 to 400 bar (Al Darouich et al., 2006). The HyPy experiments of Love et al. (1997) also show that the relative abundance of the C_{29} regular sterane was higher at a pressure of 150MPa than at the much lower 50MPa. Concomitantly, however, reduced cracking must also be linked to a higher abundance of H-donors and thence enhanced quenching of radicals. In short, a high T/K ratio serves to reduce the influence of secondary cracking on the biomarkers released by MSSV-HY.

3.2. Biomarkers in Dalong mudstone at low and high maturity

299 Having optimized MSSV-HY experimental conditions, the biomarker
300 compositions released from the kerogen samples (GY-8 and WC-4A) by MSSV-HY
301 were separately compared with those from traditional MSSV, traditional HyPy and the
302 free biomarkers in the bitumen fraction of these samples.
303
304 *3.2.1. Major organic components of free and released extractable organic matter*
305 The total ion traces of free and released saturated hydrocarbons in all samples
306 are dominated by *n*-alkanes (Fig. 7), with biomarkers also readily visible in the case
307 of the GY-8 solvent extract. For the experimental series on the GY-8 low maturity
308 kerogen the *n*-alkane distributions are similar, ranging from C_{13} to C_{35}, with neither
309 odd nor even carbon preference. There are some minor differences: MSSV and HyPy
310 both generated *n*-alkanes extending to C_{35}, whereas the range of MSSV-HY is to just
311 C_{33}.
312 For the experimental series on the over-mature WC-4A kerogen more
313 differences in composition are apparent. The *n*-alkanes detected in the solvent extract
314 ranged from C_{14} to C_{32}, maximising at C_{22}, and with a pronounced even carbon
315 predominance between C_{16} and C_{20}. Pristane and phytane are present. Isoprenoid
316 alkanes are absent from the MSSV trace, but the homologous series of *n*-alkanes from
317 C_{12} to C_{26} with an even carbon preference is readily seen. In the HyPy trace, an
318 *n*-alkane even carbon predominance is also present, with homologues extending to
319 C_{34}. Thus, there is a resemblance between MSSV and HyPy in the carbon number
320 range of these major pyrolysis products. It is therefore surprising that the MSSV-HY

yielded products extending to C_{34} but without the characteristic carbon preference. We assume that the carbon number preferences and chain lengths of first-formed *n*-alkyl radicals reflect the structure of the parent kerogen (e.g., Tegelaar et al., 1989), and that these are to varying degrees modified by radical propagation reactions (Kiran and Gillham, 1976). The data from traditional MSSV are consistent with a kerogen structure which generates *n*-alkanes with an even predominance on pyrolysis, and this predominance is also seen in the genetically associated bitumen. HyPy captures the same information. That MSSV-HY does not do so infers that non-selective cracking of *n*-alkyl radicals and olefin intermediates (Kiran and Gillham, 1976) might have been enhanced in the experiment, despite the presence of radical capping tetralin and the catalyst. The following discussions reveal that biomarker structures are released and preserved, and do not suffer from the enhanced secondary cracking reactions described here for the *n*-alkanes.

3.2.2. The distribution of hopanes

Fig. 8 shows the *m*/*z* 191 mass chromatograms for liquid hydrocarbons obtained from the samples by the stated methods. Beginning with the low maturity GY-8 sample, its free bitumen displays a full suite of C_{20}–C_{26} tricyclic terpanes and C_{29}–C_{35} 17α(H)21β(H) extended hopanes. For the MSSV products, norhopane (H_{29}) is the biggest peak; hopanes > C_{32} are essentially absent. The ratio of Tm (C_{27} 17α-trisnorhopane) to Ts (C_{27} 18α-trisnorneohopane), is commonly used as a maturity indicator (Moldowan et al., 1986). Ts was detected in the bitumen fraction of GY-8

(Ts/(Ts+Tm) = 0.17), but was absent in the products released by MSSV.

The C_{29} norhopane to C_{30} hopane ratio (H29/H30) is commonly used as source-related parameters (Peters et al., 2005). In the MSSV trace, the ratio of H29/H30 for the liquid products (1.26) is higher than that in the bitumen fraction (0.86). The distributions of hopanes in MSSV-HY and HyPy products of GY-8 are very similar but differ from the MSSV products. Ts was absent in both cases, Tm is the highest peak, closely followed by the C_{30} hopane and norhopane, and the extended hopanes up to C_{35} were detected.

The free bitumen in the over-mature sample WC-4A displays a predominance of C_{20}–C_{26} tricyclic terpanes and C_{29}–C_{31} 17α(H)21β(H) extended hopanes are also present. No hopanes were found in the MSSV products of this sample. In contrast, hopanes were detected in the MSSV-HY products. The ratio of Ts/(Ts+Tm) obtained by MSSV-HY (0.08) is much lower than that in Soxhlet extract (0.51). Previous studies have suggested that Tm was inhibited from transforming into Ts within the kerogen because the bound biomarker was protected by the macromolecular networks at relatively low maturity (Tissot and Welte, 1978; Abbott et al., 2001; Bowden et al., 2006; Meredith et al., 2008; Lockhart et al., 2008; Muhammad and Abbott, 2013). The presence of tetralin used in MSSV-HY certainly restricts the conversion of Tm to Ts, a feature also noted for the HyPy configuration (Love et al., 1995; Liao et al., 2012; Wu et al., 2013).

The relative abundance of tricyclic terpanes is very low in the liquid products released by MSSV-HY, and the same is true for HyPy. Also, C_{31}-C_{33} extended

hopanes were present in each case. Curiously, the ratio of H29/H30 obtained by MSSV-HY (2.61) is much higher that the corresponding HyPy product (0.68). This was not observed in the case of GY-8 presented above, where the ratio of H29/H30 in the MSSV-HY product (0.77) was similar to that in HyPy (0.73). Norhopane (H29) is known to be more stable than hopane (H30) at high levels of thermal maturity (Peters et al., 2005), and the high H29/H30 noted as being released by MSSV-HY is consistent with the overmaturity of the analysed sample. But it is also consistent with secondary cracking having taken place to a greater degree in MSSV-HY than in HyPy, as noted in the discussion above on *n*-alkanes. It has also to be taken into account that the decomposition level of kerogen (i.e., product yields; Table 1) is slightly higher in MSSV-HY than the closest equivalent HyPy (Table 1).

Biomarkers can be incorporated, adsorbed or absorbed into the macromolecular structure of kerogen (Snowdon et al., 2016; Cheng et al., 2016). Additionally, it is very difficult to differentiate the bound moieties released by analytical pyrolysis methods from occluded species (Snowdon et al., 2016). We conjecture that occluded biomarkers are likely to become more significant with increasing thermal maturity, because most of the covalently bound biomarkers have been depleted. In that regard, the influence of occluded biomarkers will be more severe for over-mature kerogen than mature kerogen. To what degree occlusion has occurred is not known, but the abundance of C_{30} hopane in both the free bitumen and HyPy products is noted.

387 *3.2.3 The distribution of steranes*

388 Fig. 9 shows the *m*/*z* 217 mass chromatograms for liquid hydrocarbons
389 obtained from two kerogens by the different analytical methods used here. Beginning
390 with the low mature sample GY-8, only regular steranes are present; diasteranes were
391 not detected in any analysis of GY-8. The relative abundances of C_{27}–C_{29} ααα*R*
392 steranes in the Soxhlet extract are $C_{27} \approx C_{29} > C_{28}$, whereas a strong C_{27}
393 predominance ($C_{27} > C_{29} > C_{28}$) is noted for the MSSV products. The ratios of
394 C29-ββ/(ββ+αα) and C29-20S/(20S+20R) are slightly lower for MSSV products than
395 they are in the corresponding source rock extract (Table 3). The relative abundance of
396 diginane and 20-methyldiginane, given as the ratio S21/S22, is much higher for the
397 MSSV product (3.02) than for the solvent extract (1.2). As far as MSSV-HY is
398 concerned, the relative abundances of C_{27}–C_{29} ααα*R* steranes are $C_{27} \approx C_{29} > C_{28}$,
399 this being similar to those noted for the solvent extract but strongly dissimilar to those
400 of MSSV. A very similar distribution was seen for reference HyPy products. The
401 ratios of C29-ββ/(ββ+αα) and C29-20S/(20S+20R) in products released by both
402 MSSV-HY and HyPy are also slightly lower than those in their corresponding extract
403 of source rock (Table 3), and the ratio of S21/S22 for the liquid products of
404 MSSV-HY (1.62) is similar to that in bitumen fraction (1.2).

405 For the over-mature sample WC-4A, the distributions of C_{27}–C_{29} regular
406 steranes in the Soxhlet extract (free phase) exhibit a strong C_{27} predominance ($C_{27} >$
407 $C_{29} \approx C_{28}$) due to the influence of high thermal maturity. In that regard, significant
408 contributions of diasteranes were also detected in the Soxhlet extract. While steranes

were completely absent in the MSSV products of this over-mature sample, they were detected in MSSV-HY, exhibiting $C_{29} > C_{27} > C_{28}$ abundances. Similar abundances were noted for HyPy products. Trace amounts of diasteranes are found in the liquid products obtained by HyPy, but are absent in the MSSV-HY product. The more significant contribution of occluded biomarkers in HyPy product cannot be ruled out, as discussed for the case of hopanes. The absence or trace abundance of diasteranes may be due to the lower thermal maturity of the MSSV-HY and HYPY released kerogen fractions (cf. free hydrocarbons of bitumen fraction). Thus, for both the mature and over-mature kerogens under study, the steranes released by MSSV-HY bear a general resemblance to those obtained by HyPy.

4. Conclusions

In contrast to MSSV alone, whose pyrolysate biomarker components are strongly affected by secondary cracking reactions, the presence of tetralin and catalyst in the reactor (MSSV-HY) reduces the influence of secondary cracking considerably. The best conditions for releasing and preserving biomarkers from kerogen using MSSV-HY is a combination of temperature (400 °C), heating time (120 min), high tetralin: kerogen ratio (5:1), and the use of a dispersed sulfide molybdenum catalyst.

A comparison of biomarker distributions released from the two Dalong Formation kerogen (low maturity and over-mature) samples using MSSV and MSSV-HY has confirmed the effectiveness of the new method. Compositions from MSSV-HY are similar to, though not identical with, those released by the established

HyPy technique.

This proof of concept study has shown that off-line microscale sealed vessel catalytic hydrogenation (MSSV-HY) shows great promise for applications in petroleum geochemistry. In particular, MSSV-HY, which represents a combination of MSSV and HyPy concepts could allow paleoenvironment to be assessed and compositional kinetic models to be built using the same pyrolysis system. The utility of MSSV-HY for studies of young sediments has yet to be investigated.

Acknowledgements

This work was supported by the National Foundation of China (Grant No. 41673044) and the laboratory infrastructure at GFZ German Research Centre for Geosciences. We thank Ferdinand Perssen for his excellent technical assistance with the MSSV experiments. We are grateful to Cornelia Karger for GC–MS analysis, Anke Kaminsky and Kristin Günther for laboratory assistance, and Dr. Rene Jarling for discussions. The Special Fund for the Strategic Priority Research Program of the Chinese Academy of Sciences Grant No. XDA14010103 and the National Science and Technology Major Project Grant No. 2017ZX05008-002 are acknowledged for the continuing support of Wu's MSSV research in Guangzhou. This is contribution No. IS-2603 from GIGCAS. Dr. Will Meredith and an anonymous reviewer are gratefully acknowledged for their constructive comments and suggestions. We are particularly grateful to Dr. Paul Greenwood (Associate Editor), whose attention to detail and helpful suggestions were instrumental in improving the paper significantly. We also

thank Dr. John Volkman for his help and advice.

Associate Editor–**Paul Greenwood**

Reference

Abbott, G.D., Bennett, B., Petch, G.S., 1995. The thermal degradation of 5α(H)-cholestane during closed-system pyrolysis. Geochimica et Cosmochimica Acta 59, 2259–2264.

Abbott, G.D., Bashir, F.Z., Sugden, M.A., 2001. Kerogen-bound and free hopanoic acids in the messel oil shale kerogen. Chirality 13, 510–516.

Adam, P., Schmid, J.C., Mycke, B., Strazielle, C., Connan, J., Huc, A., Riva, A., Albrecht, P., 1993. Structural investigations of nonpolar sulfur cross-linked macromolecules in petroleum. Geochimica et Cosmochimica Acta 57, 3395–3419.

Al Darouich, T., Behar, F., Largeau, C., 2006. Pressure effect on the thermal cracking of the light aromatic fraction of Safaniya crude oil – Implications for deep prospects. Organic Geochemistry 37, 1155–1169.

Behar, F., Pelet, R., Roucache, J., 1984. Geochemistry of asphaltenes. Organic Geochemistry 6, 587–595.

Berwick, L., Greenwood, P., Kagi, R., Croué, J., 2007. Thermal release of nitrogen organics from natural organic matter using micro scale sealed vessel pyrolysis. Organic Geochemistry 38, 1073–1090.

Berwick, L.J., Greenwood, P.F., Meredith, W., Snape, C.E., Talbot, H.M., 2010.

475 Comparison of microscale sealed vessel pyrolysis (MSSVpy) and
476 hydropyrolysis (Hypy) for the characterization of extant and sedimentary
477 organic matter. Journal of Analytical and Applied Pyrolysis 87, 108–116.
478 Berwick, L., Alexander, R., Pierce, K., 2011. Formation and reactions of alkyl
479 adamantanes in sediments: Carbon surface reactions. Organic Geochemistry 42,
480 752–761.
481 Bevanente, E., Santa Ana, M.A., Mendizábal, F., Gonzáler, G., 2002. Interaction
482 chemistry of molybdenum disulfide. Coordination Chemistry Reviews 24,
483 87–109.
484 Boone, W.P., Ekerdt, J.G., 2000. Hydrodesulfurization studies with a single-layer
485 molybdenum disulfide catalyst. Journal of Catalysis 193, 96–102.
486 Bowden, S.A., Farrimond, P., Snape, C.E., Love, G.D., 2006. Compositional
487 differences in biomarker constituents of the hydrocarbon, resin, asphaltene and
488 kerogen fractions: an example from the jet rock (Yorkshire, UK). Organic
489 Geochemistry 37, 369–383.
490 Brown, S.D., Sirkecioglu, O., Ismail, K., Andresen, J.M., Snape, C.E., Buchanan, III
491 A.C., Britt, P.F., 1994. Use of hydropyrolysis – MS to probe the hydrocracking
492 of diphenylalkane linkages in the solid state. Preprints American Chemical
493 Society Division of Fuel Chemistry 39, 801–805.
494 Cheng, B., Du, J.Y., Tian, Y.K., Liu, H., Liao, Z.W., 2016. Thermal evolution of
495 adsorbed/occluded hydrocarbons inside kerogens and its significance as
496 exemplified by one low-matured kerogen from Santanghu Basin, Northwest

China. Energy & Fuels 30, 4529–4536.

Comet, P.A., McEvoy, J., Giger, W., Douglas, A.G., 1986. Hydrous and anhydrous pyrolysis of DSDP Leg 75 kerogens – A comparative study using a biological marker approach. Organic Geochemistry 9, 171–182.

Dieckmann, V., Horsfield, B., Schenk, H.J., Welte, D.H., 1998. Kinetics of petroleum generation and cracking by programmed-temperature closed-system pyrolysis of Posidonia Shale. Fuel 77, 23–31.

Eglinton, T.I., Douglas, A.G., 1988. Quantitative study of biomarker hydrocarbons released from kerogens during hydrous pyrolysis. Energy & Fuels 2, 81–88.

Farag, H., EI-Hendawy, A.N.A., Sakanishi, K., Kishida, M., Mochida, I., 2009. Catalytic activity of synthesized nanosized molybdenum disulfide for the hydrodesulfurization of dibenzothiophene: Effect of H_2S partial pressure. Applied Catalysis B: Environmental 91, 189–197.

Gallegos, E.J., 1975. Terpane-sterane release from kerogen by pyrolysis gas chromatography-mass spectrometry. Analytical Chemistry 47, 1524–1528.

Gates, B.C., 1979. Liquefied coal by hydrogenation. Chemischer Informationsdienst 10, 97–102.

Greenwood, P.F., Leenheer, J.A., Berwick, L.J., Franzmann, P., 2006. Bacterial biomarkers thermally released from dissolved organic matter. Organic Geochemistry 37, 597–609.

Hamann, S.D., 1963. Chemical kinetics. In: Bradley, R.S. (Ed.), High Pressure Physics and Chemistry. Academic Press, London, pp. 163–207.

519 He, K., Zhang, S.C., Mi, J.K., Chen, J.P., Cheng, L., 2011. Mechanism of catalytic
520 hydropyrolysis of sedimentary organic matter with MoS_2. Petroleum Science 8,
521 134–142.
522 Hoffman, I.C., Hutchison, J., Robson, J.N., Chicarelli, M.I., Maxwell, J.R., 1992.
523 Evidence for sulphide links in a crude oil asphaltene and kerogens from
524 reductive cleavage by lithium in ethylamine. Organic Geochemistry 19,
525 371–387.
526 Horsfield, B., Disko, U., Leistner, F., 1989. The micro-scale simulation of maturation:
527 Outline of a new technique and its potential applications. Geologische
528 Rundschau 78, 361–374.
529 Horsfield, B., Schenk, H.J., Mills, N., Welte, D.H., 1992. An investigation of the
530 in-reservoir conversion of oil to gas: compositional and kinetic findings from
531 closed-system programmed-temperature pyrolysis. Organic Geochemistry 19,
532 191–204.
533 Horsfield, B., Leistner, F., Hall, K., 2015. Microscale Sealed Vessel Pyrolysis. In:
534 Grice K. (Ed.), Principles and Practice of Analytical Techniques in Geosciences.
535 Royal Society Chemistry Detection Science Series 4, 209–250.
536 Huang, D.F., Zhang, D.J., Li, J.C., 1994. The origin of 4-methyl steranes and
537 pregnanes from Tertiary strata in the Qaidam Basin, China. Organic
538 Geochemistry 22, 343–348.
539 Keym, M., Dieckmann, V., Horsfield, B., Erdmann, M., Galimberti, R. Kua, L.C.,
540 Leith, L., Podlaha, O., 2006. Source rock heterogeneity of the Upper Jurassic

Draupne Formation, North Viking Graben, and its relevance to petroleum generation studies. Organic Geochemistry 37, 220–243.

Kiran, P., Gillham, J.G., 1976. Pyrolysis-molecular weight chromatography: a new on-line system for analysis of polymers. II. Thermal decomposition of polyolefins – polyethylene, polypropylene, polyisobutane. Journal Applied Polymer Science 20, 2045–2068.

Koopmans, M.P., Carson, F.C., Sinninghe Damsté, J.S., Lewan, M.D., 1998. Biomarker generation from Type II-S kerogens in claystone and limestone during hydrous and anhydrous pyrolysis. Organic Geochemistry 29, 1395–1402.

de Leeuw, J.W., Cox, H.C., van Graas, G., van de Meer, F.W., Peakman, T.M., Baas, J.M.A., van de Graaf, B., 1989. Limited double bond isomerization and selective hydrogenation of sterenes during early diagenesis. Geochimica et Cosmochimica Acta 53, 903–909.

Lewan, M.D., 1997. Experiments on the role of water in petroleum formation. Geochimica et Cosmochimica Acta 61, 3691–3723.

Liao, Y.H., Fang, Y.X., Wu, L.L., Geng, A.S., Hsu, C.S., 2012. The characteristics of the biomarkers and $\delta^{13}C$ of *n*-alkanes released from thermally altered solid bitumens at various maturities by catalytic hydropyrolysis. Organic Geochemistry 46, 56–65.

Lockhart, R.S., Meredith, W., Love, G.D., Snape, C.E., 2008. Release of bound aliphatic biomarker via hydropyrolysis from Type II kerogen at high maturity. Organic Geochemistry 39, 1119–1124.

563 Love, G.D., Snape, C.E., Carr, A.D., Houghton, R., 1995. Release of bound alkane
564 biomarkers in high yields from kerogen via catalytic hydropyrolysis. Organic
565 Geochemistry 23, 981–986.
566 Love, G.D., Snape, C.E., Carr, D.A., Houghton, R.C., 1996. Changes in molecular
567 biomarker and bulk carbon skeletal parameters of vitrinite concentrates as a
568 function of rank. Energy & Fuels 10, 149–157.
569 Love, G.D., McAulay, A., Snape, C.E, Bishop, A.N., 1997. Effect of process variable
570 in catalytic hydropyrolysis on the release of bound aliphatic hydrocarbons from
571 sedimentary organic matter. Energy & Fuels 11, 522–531.
572 Meredith, W., Snape, C.E., Carr, A.D., Nytoft, H.P., Love, G.D., 2008. The occurrence
573 of unusual hopanes in hydropyrolysates generated from severely biodegraded
574 oil seep asphaltenes. Organic Geochemistry 39, 1243–1248.
575 Michels, R., Landais, P., Philp, R.P., Torkelson, B.E., 1994. Effects of pressure on
576 organic matter maturation during confined pyrolysis of Woodford kerogen.
577 Energy & Fuels 8, 741–754.
578 Moldowan, J.M., Sundararaman, P., Schoell, M., 1986. Sensitivity of biomarker
579 properties to depositional environment and/or source input in the Lower
580 Toarcian of SW-Germany. Organic Geochemistry 10, 915–926.
581 Muhammad, A.B., Abbott, G.D., 2013. The thermal evolution of asphaltene-bound
582 biomarkers from coals of different rank: A potential information resource during
583 coal biodegradation. International Journal of Coal Geology 107, 90–95.
584 Murray, I.P., Love, G.D., Snape, C.E., Bailey, N.J.L., 1998. Comparison of

585 covalently-bound aliphatic biomarkers released via hydropyrolysis with their
586 solvent-extractable counterparts for a suite of Kimmeridge clays. Organic
587 Geochemistry 29, 1487–1505.
588 Mycke, B., Narjes, F., Michaelis, W., 1987. Bacteriohopanetetrol from chemical
589 degradation of an oil shale kerogen. Nature 326, 179–181.
590 Peters, K.E., Walters, C.C., Moldowan, J.M., 2005. The Biomarker Guide,
591 Biomarkers and Isotopes in Petroleum Exploration and Earth history.
592 Cambridge University Press, New York.
593 di Primio, R., Horsfield, B., 2006. From petroleum-type organofacies to hydrocarbon
594 phase prediction. American Association of Petroleum Geologists Bulletin 90,
595 1031–1058.
596 Radke, M., Schaefer, R.G., Leythaeuser, D., Teichmüller, M., 1980. Composition of
597 soluble organic matter in coals: relation to rank and liptinite fluorescence.
598 Geochimica et Cosmochimica Acta 44, 1787–1800.
599 Richnow, H.H., Jenisch, A., Michaelis, W., 1992. Structural investigations of sulphur
600 rich macromolecular oil fractions and a kerogen by sequential chemical
601 degradation. Organic Geochemistry 19, 351–370.
602 Rubinstein, I., Spyckerelle, C., Strausz, O.P., 1979. Pyrolysis of asphaltenes: A source
603 of geochemical information. Geochimica et Cosmochimica Acta 43, 1–6.
604 Russell, R.A., Snape, C.E., Meredith, W., Love, G.D., Clarke, E., Moffatt, B., 2004.
605 The potential of bound biomarker profiles released via catalytic hydropyrolysis
606 to reconstruct basin charging history for oils. Organic Geochemistry 35,

607 1441–1459.
608 Schenk, H.J., di Primio, R., Horsfield, B., 1997. The conversion of oil into gas. Part 1:
609 Comparative kinetic investigation of gas generation from crude oils of lacustrine,
610 marine and fluviodeltaic origin by programmed-temperature closed-system
611 pyrolysis. Organic Geochemistry 26, 467–481.
612 Seifert, W.K., 1978. Steranes and terpanes in kerogen pyrolysis for correlation of oils
613 and source rocks. Geochimica et Cosmochimica Acta 42, 473–484.
614 Seifert, W.K., Moldowan, J.M., 1980. The effect of thermal stress on source-rock
615 quality as measured by hopane stereochemistry. Physics and Chemistry of the
616 Earth 12, 229–237.
617 Shi, X.R., Jiao, H.J., Hermann, K., Wang, J.G., 2009. CO hydrogenation reaction on
618 sulfided molybdenum catalysts. Journal of Molecular Catalysis A: Chemical 312,
619 7–17.
620 Snowdon, L.R., Volkman, J.K., Zhang, Z.R., Tao, G.L., Liu, P., 2016. The organic
621 geochemistry of asphaltenes and occluded biomarkers. Organic Geochemistry
622 91, 3–15.
623 Sundaram, H.S., Given, P.H., 1983. Characterization of artifacts produced from
624 tetralin donor vehicle under coal liquefaction conditions. Preprints American
625 Chemical Society Division of Fuel Chemistry 28, 26.
626 Tegelaar, E.W., Matthezing, R.M., Jansen, B.H., Horsfield, B., de Leeuw, J.W., 1989.
627 Possible origin of n-alkanes in high-wax crude oils. Nature 342, 529–531.
628 Tissot, B.P., Welte, D.H., 1978. Petroleum Formation and Occurrence: A new

629 Approach to Oil and Gas Exploration. Springer-Verlag.
630 Vlieger, J.J.D., 1988. Aspects of the chemistry of hydrogen donor solvent coal
631 liquefaction. Applied Sciences 43, 228–255.
632 Wang, G.L., Chang, X.C., Wang, T.G., Simoneit, B.R.T., 2015. Pregnanes as molecular
633 indicators for depositional environments of sediments and petroleum source
634 rocks. Organic Geochemistry 78, 110–120.
635 Wilhelms, A., Larter, S.R., Leythaeuser, D. 1991. Influence of bitumen-2 on
636 Rock-Eval pyrolysis. Organic Geochemistry 17, 351–354.
637 Wingert, W., Pomerantz, M., 1986. Structure and significance of some twenty-one and
638 twenty-two carbon petroleum steranes. Geochimica et Cosmochimica Acta 50,
639 2763–2769.
640 Wu, L.L., Liao, Y.H., Fang, Y.X., Geng, A.S., 2012. The study on the source of the oil
641 seeps and bitumens in the Tianjiangshan structure of the northern Longmen
642 Mountain structure of Sichuan Basin, China. Marine and Petroleum Geology 37,
643 147–161.
644 Wu, L.L., Liao, Y.H., Fang, Y.X., Geng, A.S., 2013. The comparison of biomarkers
645 released by hydropyrolysis and Soxhlet extraction from source rocks of different
646 maturities. Chinese Science Bulletin 58, 373–383.
647 Wu, L.L., Geng, A.S., 2016. Differences in the thermal evolution of hopanes and
648 steranes in free and bound fractions. Organic Geochemistry 101, 38–48.
649 Yang, S.Y., Horsfield, B., 2016. Some predicted effects of minerals on the generation
650 of petroleum in nature. Energy & Fuels 30, 6677–6687.

651 Zelenski, C.M, Dorhout, P.K., 1998. Template synthesis of near-monodisperse
652 microscale nanofibers and nanotubes of MoS_2. Journal of American Chemical
653 Society 120, 734–742.
654

Figure Captions:

Fig. 1. The total *n*-alkanes and total hopanes yields of MSSV pyrolysis products at various conditions.

Fig. 2. Total ion chromatogram for the liquid products of pyrolysis for kerogen and tetralin, neat kerogen, and neat tetralin at 400 °C for 120 mins.

Fig. 3. The *m*/*z* 191 and *m*/*z* 217 chromatograms of products obtained from the MSSV experiment of the GY-8 kerogen alone, kerogen with catalyst, kerogen with tetralin, and MSSV-HY experiment of kerogen. S21= diginane (5α,14β,17β(H)-pregnane); S22 = 20-methyldiginane (5α,14β,17β(H)-homopregnane); C27 = C_{27} ααα20R cholestane; C28 = C_{28} ααα20R ergostane; C29 =C_{29} ααα20R stigmastane; TT20–TT26 = C_{20}–C_{26} tricyclic terpanes; tT24 = C_{24} tetracyclic terpanes; Ts = C_{27} 18α-trisnorneohopane; Tm = C_{27} 17α-trisnorhopane; H29–H33 = C_{29}–C_{33} 17α(H)21β(H)-hopanes; Gam = gammacerane.

Fig. 4. The *m*/*z* 191 and *m*/*z* 217 chromatograms of products released by MSSV-HY from the low maturity GY-8 kerogen at various tetralin:kerogen ratios (T/K).

Fig. 5. The evolution trend of (S21+S22)/(C_{27} +C_{28}+C_{29}) regular steranes ratio with T/K ratio from the MSSV-HY experiments of the low maturity GY-8 kerogen.

Fig. 6. The distribution of regular C_{27}–C_{29} steranes for liquid products released from the low maturity GY-8 kerogen by MSSV-HY with different T/K ratios, and HyPy.

Fig. 7. The distribution of total ion traces of free and released organic components from the low maturity GY-8 kerogen and the high maturity WC-4A kerogen.

677 **Fig. 8**. The *m*/*z* 191 chromatograms of free and released organic components from the
678 low maturity GY-8 kerogen and the high maturity WC-4A kerogen.
679 **Fig. 9**. The *m*/*z* 217 chromatograms of free and released organic components from the
680 low maturity GY-8 kerogen and the high maturity WC-4A kerogen.

Table 1. Total extract, saturates, aromatic fraction yields and *n*-alkanes and total hopanes yields from MSSV, MSSV-HY and HyPy experiments of GY-8 kerogen.

	Conditions		Yield, mg of extract/g TOC of kerogen			Yield, μg/g TOC of kerogen	
Test No.	Additive	T/K ratio	saturates	aromatics	∑DCM solubles	Total *n*-alkanes	Total hopanes
MSSV-1	-	-	39	56	385	1066	10.9
MSSV-2	Catalyst	-	37	62	392	1089	12.8
MSSV-3	Tetralin	-	45	57	416	1157	12.8
MSSV-HY-1	Catalyst+Tetralin	1:2	55	59	754	2081	65.9
MSSV-HY-2	Catalyst+Tetralin	1:1	70	73	1085	1892	87.0
MSSV-HY-3	Catalyst+Tetralin	2:1	48	68	1169	1832	123.1
MSSV-HY-4	Catalyst+Tetralin	5:1	66	71	1037	2137	137.8
HyPy-1	Catalyst	-	110	166	498	-	-

Note: "-" mean undetectable, ∑DCM solubles for MSSV is over 1000 for some experiments because some products from tetralin (such as binaphthalenes) existed in MSSV-HY product, total extract, saturates, aromatic fractions were weighted using a high performance balance with a precision of 0.01mg.

Table 2. The biomarker parameters in products released from GY-8 kerogen by MSSV and MSSV-HY.

Biomarker parameters	MSSV			MSSV-HY			
	MSSV-1	MSSV-2	MSSV-3	MSSV-HY-1	MSSV-HY-2	MSSV-HY-3	MSSV-HY-4
C27/(C27+ C28+ C29)	58	48	36	55	52	50	38
C28/(C27+ C28+ C29)	22	31	36	24	24	22	22
C29/(C27+ C28+ C29)	20	21	27	21	24	28	40
S21/S22	3.02	3.23	3.15	1.84	1.86	1.82	1.62
C27 βαR/C27ααR	-	-	-	-	-	-	-
C29-ββ/(ββ+αα)	0.49	0.53	0.32	0.6	0.59	0.58	0.45
C29-20S/(20S+20R)	0.4	0.41	0.53	0.4	0.41	0.43	0.42
Ts/(Ts+Tm)	-	-	-	-	-	-	-
TT23/(TT23+tT24)	0.49	0.39	0.71	0.61	0.6	0.58	0.60
TT23/H30	0.31	0.25	0.79	0.17	0.15	0.17	0.15
H29/H30	1.26	1.28	1.74	0.77	0.75	0.76	0.77
H31-22S/(22S+22R)	0.56	0.53	0.56	0.54	0.51	0.57	0.55
Gam/H30	-	-	-	0.13	0.11	0.12	0.11
(S21+S22)/ (C_{27}+C_{28}+C_{29}) regular steranes	0.72	0.69	0.82	0.68	0.48	0.36	0.23

Note: “-” means undetectable; (S21+S22)/ (C_{27}+C_{28}+C_{29}) regular steranes: (diginane +20-methyldiginane)/ C_{27}–C_{29} regular steranes (12 peaks).

Table 3. The biomarker parameters in extract from original source rocks and products released by MSSV, MSSV-HY and HyPy technique.

Biomarker parameters	GY-8 (*R*o: 0.6%)				WC-4A (*R*o: 1.8%)			
	Soxh	MSSV	MSSV-HY	HyPy	Soxh	MSSV	MSSV-HY	HyPy
C27/(C27+ C28+ C29)	43	58	38	34	46	-	42	33
C28/(C27+ C28+ C29)	20	22	22	21	30	-	10	12
C29/(C27+ C28+ C29)	38	20	40	45	24	-	48	55
S21/S22	1.2	3.02	1.62	1.42	1.85	-	1.27	1.69
C27 βαR/C27ααR	0.08	-	-	-	0.44	-	-	0.19
C29S-ββ/(ββ+αα)	0.57	0.49	0.45	0.42	0.40	-	0.34	0.40
C29-20S/(20S+20R)	0.45	0.4	0.42	0.44	0.57	-	0.43	0.14
Ts/(Ts+Tm)	0.17	-	-	-	0.51	-	0.08	0.27
TT23/(TT23+TT24)	0.59	0.49	0.60	0.64	0.64	-	0.67	0.69
TT23/H30	0.11	0.31	0.15	0.12	1.19	-	0.52	0.52
H29/H30	0.86	1.26	0.77	0.73	0.66	-	2.61	0.68
H31-22S/(22S+22R)	0.6	0.56	0.55	0.6	0.60	-	0.62	0.60
Gam/H30	0.09	-	0.11	0.09	-	-	-	-
(S21+S22)/ (C_{27}+C_{28}+C_{29}) regular steranes	0.21	0.72	0.23	0.13	0.29	-	0.21	0.09

Note: “-” means undetectable.

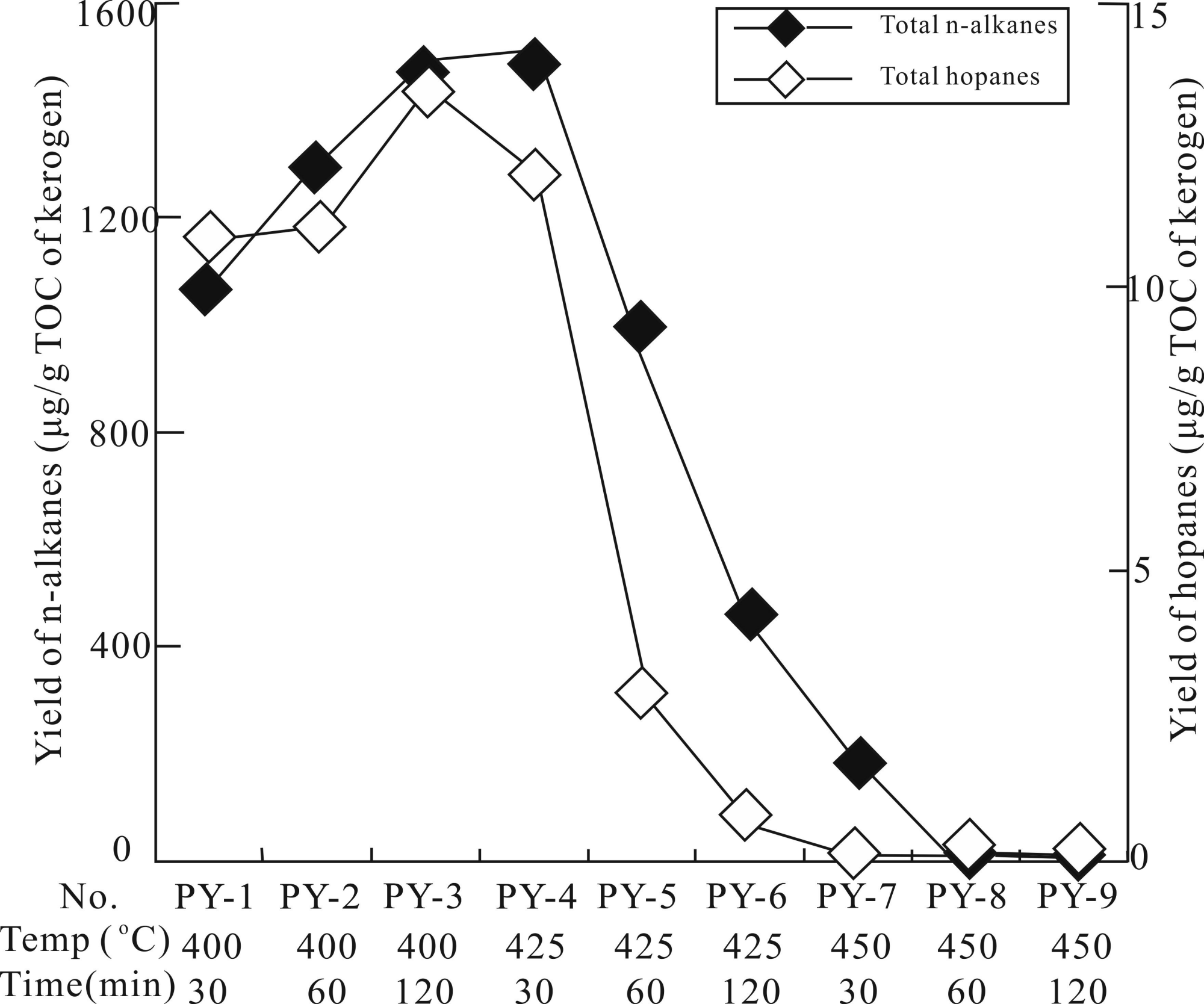
Total n-alkanes
Total hopanes
Yield of n-alkanes (μg/g TOC of kerogen)
Yield of hopanes (μg/g TOC of kerogen)
1600
1200
800
400
0
15
10
5
0
No. PY-1 PY-2 PY-3 PY-4 PY-5 PY-6 PY-7 PY-8 PY-9
Temp (°C) 400 400 400 425 425 425 450 450 450
Time(min) 30 60 120 30 60 120 30 60 120

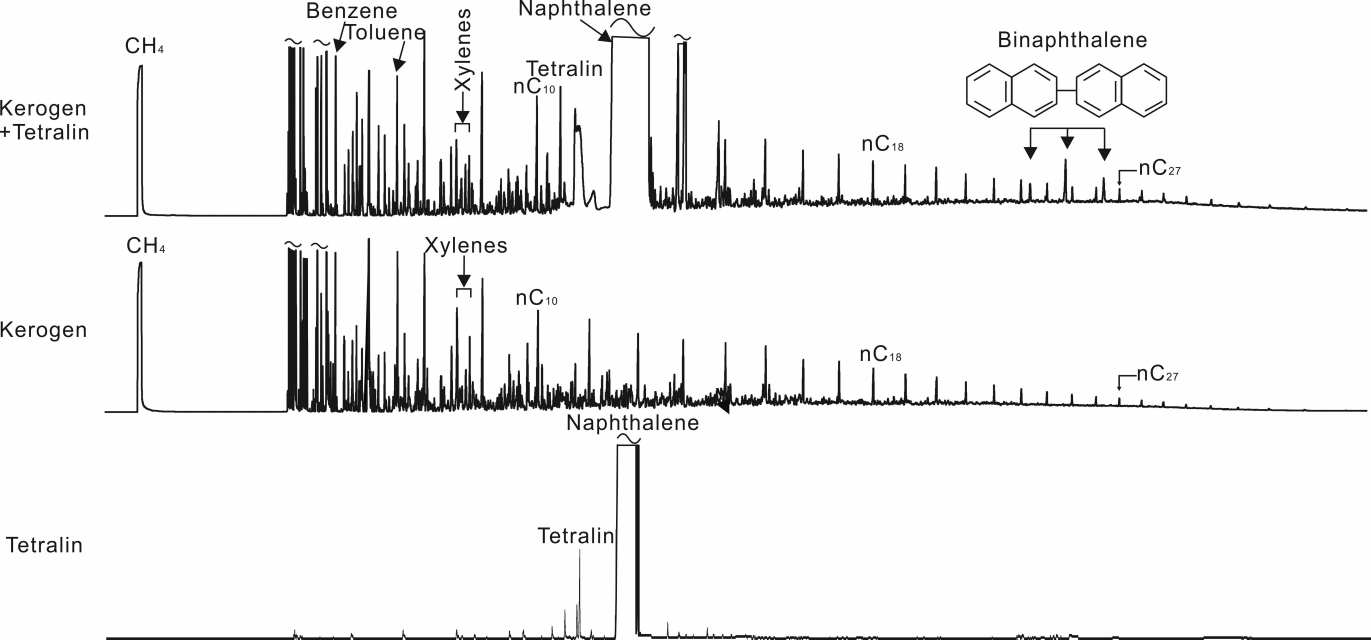
Kerogen +Tetralin
CH4
Benzene
Toluene
Xylenes
Naphthalene
Tetralin
nC10
nC18
nC27
Binaphthalene
Kerogen
CH4
Xylenes
nC10
nC18
nC27
Naphthalene
Tetralin
Tetralin

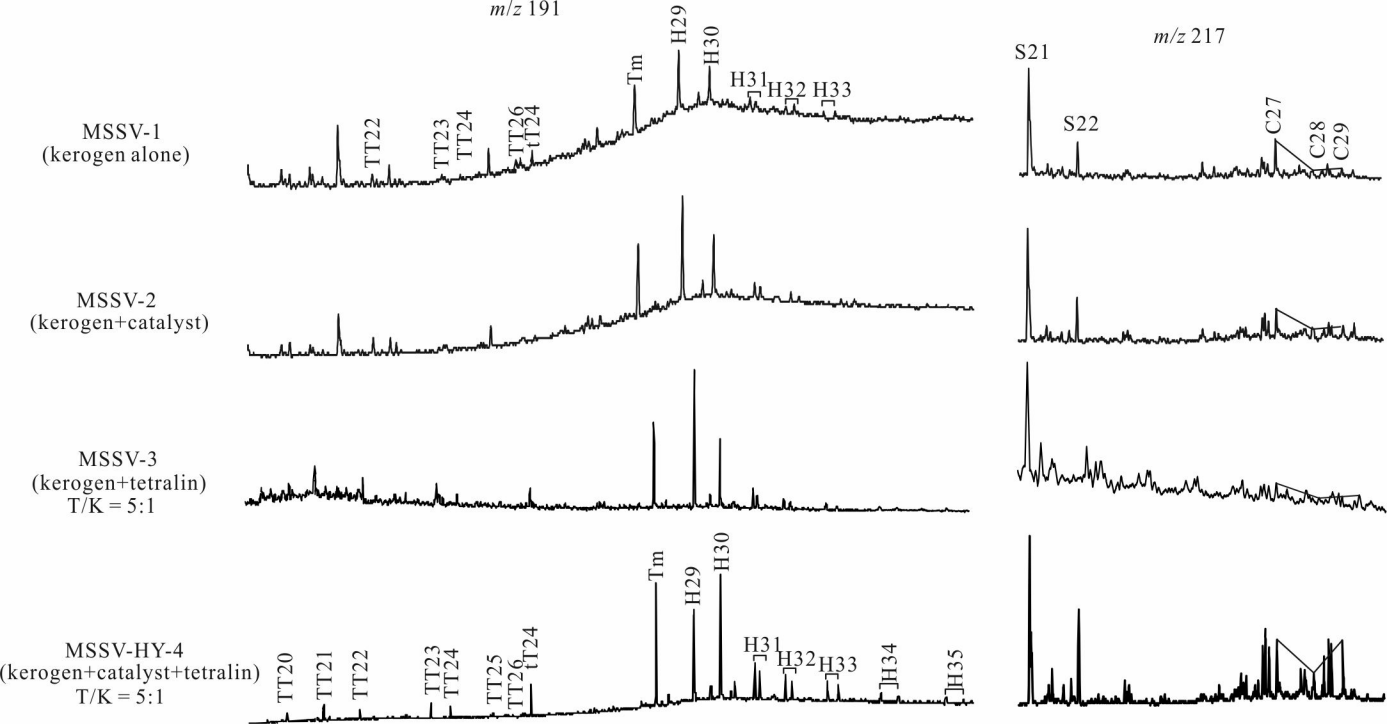
m/z 191
m/z 217
MSSV-1
(kerogen alone)
MSSV-2
(kerogen+catalyst)
MSSV-3
(kerogen+tetralin)
T/K = 5:1
MSSV-HY-4
(kerogen+catalyst+tetralin)
T/K = 5:1
TT20
TT21
TT22
TT23
TT24
TT25
TT26
tT24
Tm
H29
H30
H31
H32
H33
H34
H35
S21
S22
C27
C28
C29

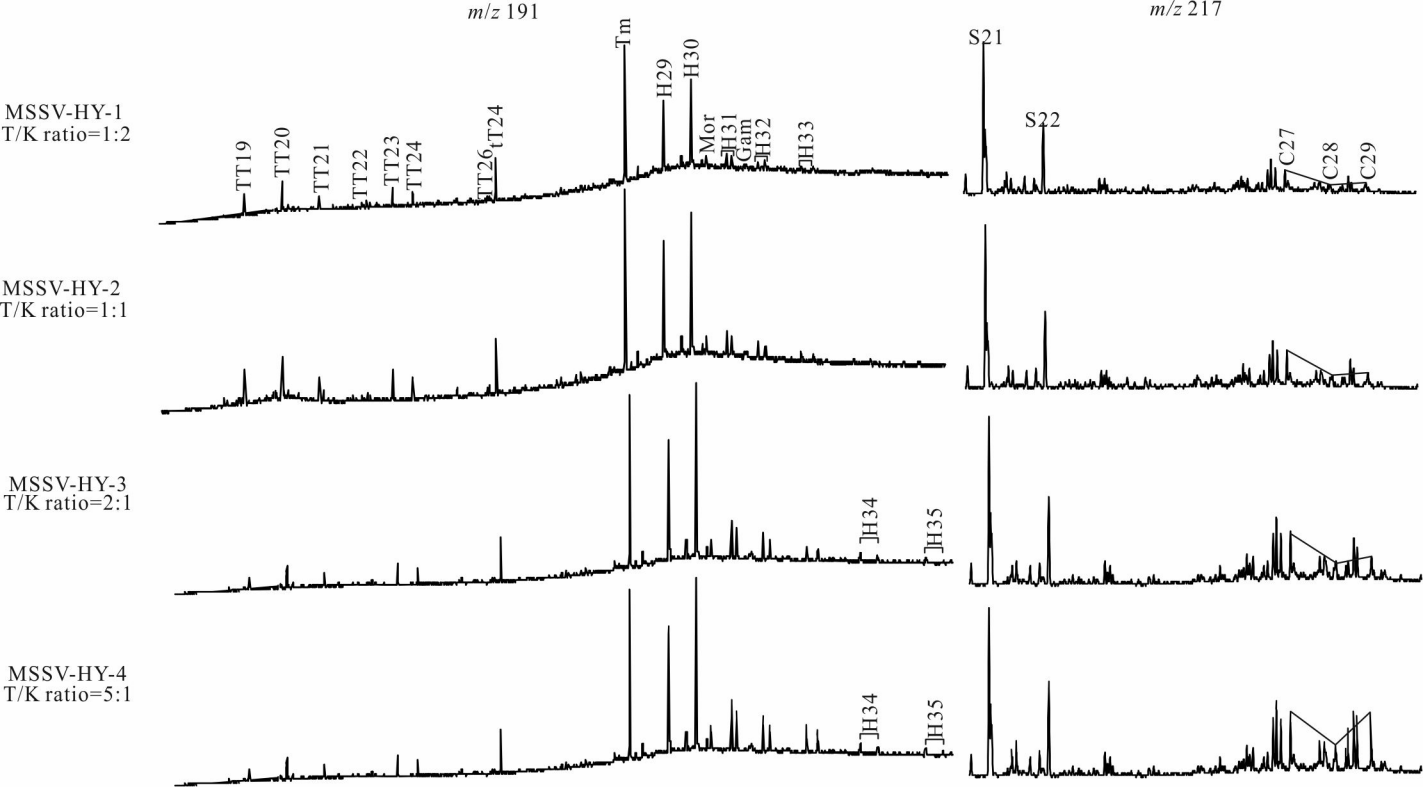
m/z 191
m/z 217
MSSV-HY-1
T/K ratio=1:2
MSSV-HY-2
T/K ratio=1:1
MSSV-HY-3
T/K ratio=2:1
MSSV-HY-4
T/K ratio=5:1
TT19
TT20
TT21
TT22
TT23
TT24
TT26
tT24
Tm
H29
H30
Mor
H31
Gam
H32
H33
H34
H35
S21
S22
C27
C28
C29

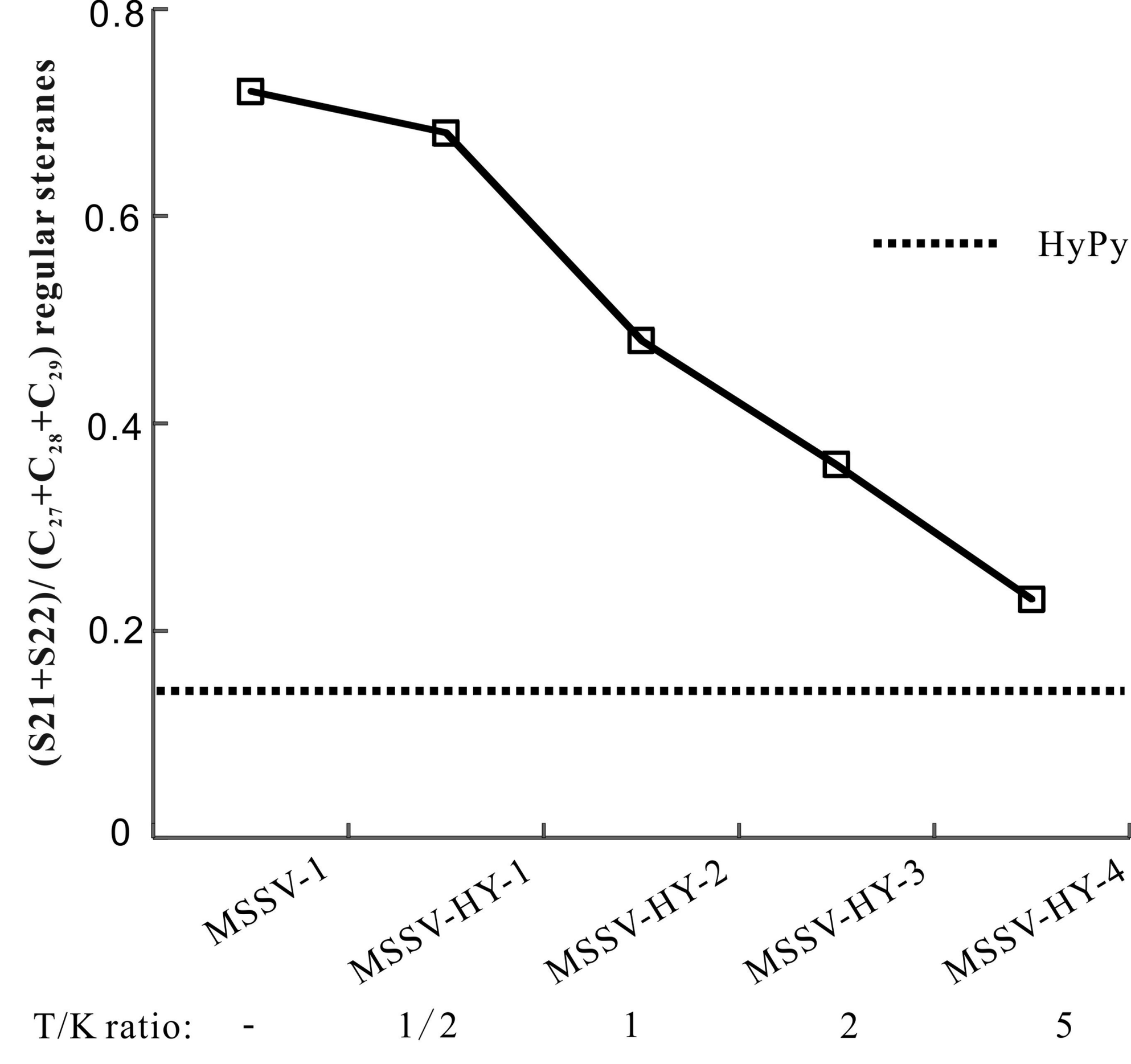
0.8
0.6
0.4
0.2
0
(S21+S22)/ (C27+C28+C29) regular steranes
HyPy
MSSV-1
MSSV-HY-1
MSSV-HY-2
MSSV-HY-3
MSSV-HY-4
T/K ratio: - 1/2 1 2 5

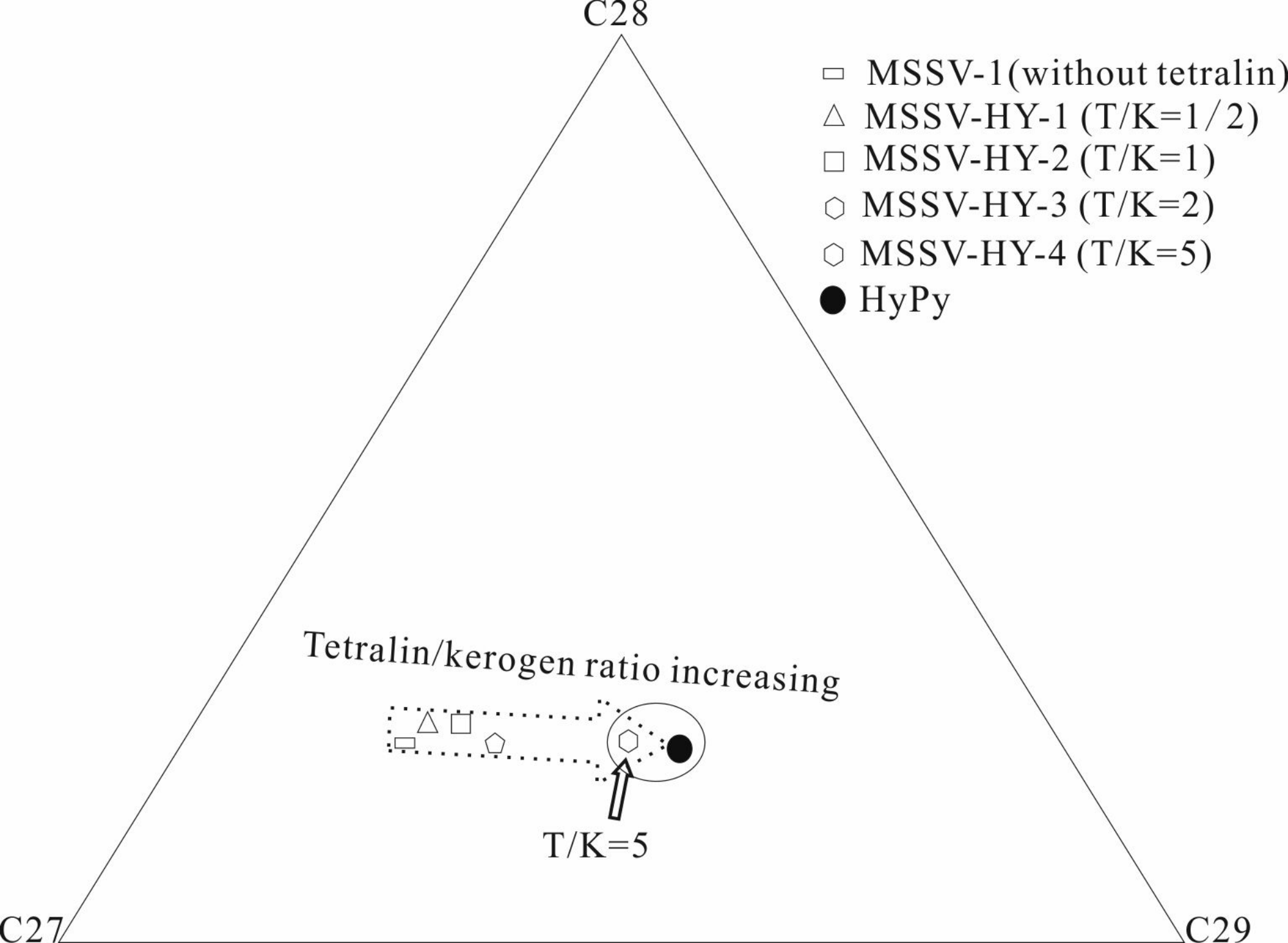
C28
C27
C29
MSSV-1(without tetralin)
MSSV-HY-1 (T/K=1/2)
MSSV-HY-2 (T/K=1)
MSSV-HY-3 (T/K=2)
MSSV-HY-4 (T/K=5)
HyPy
Tetralin/kerogen ratio increasing
T/K=5

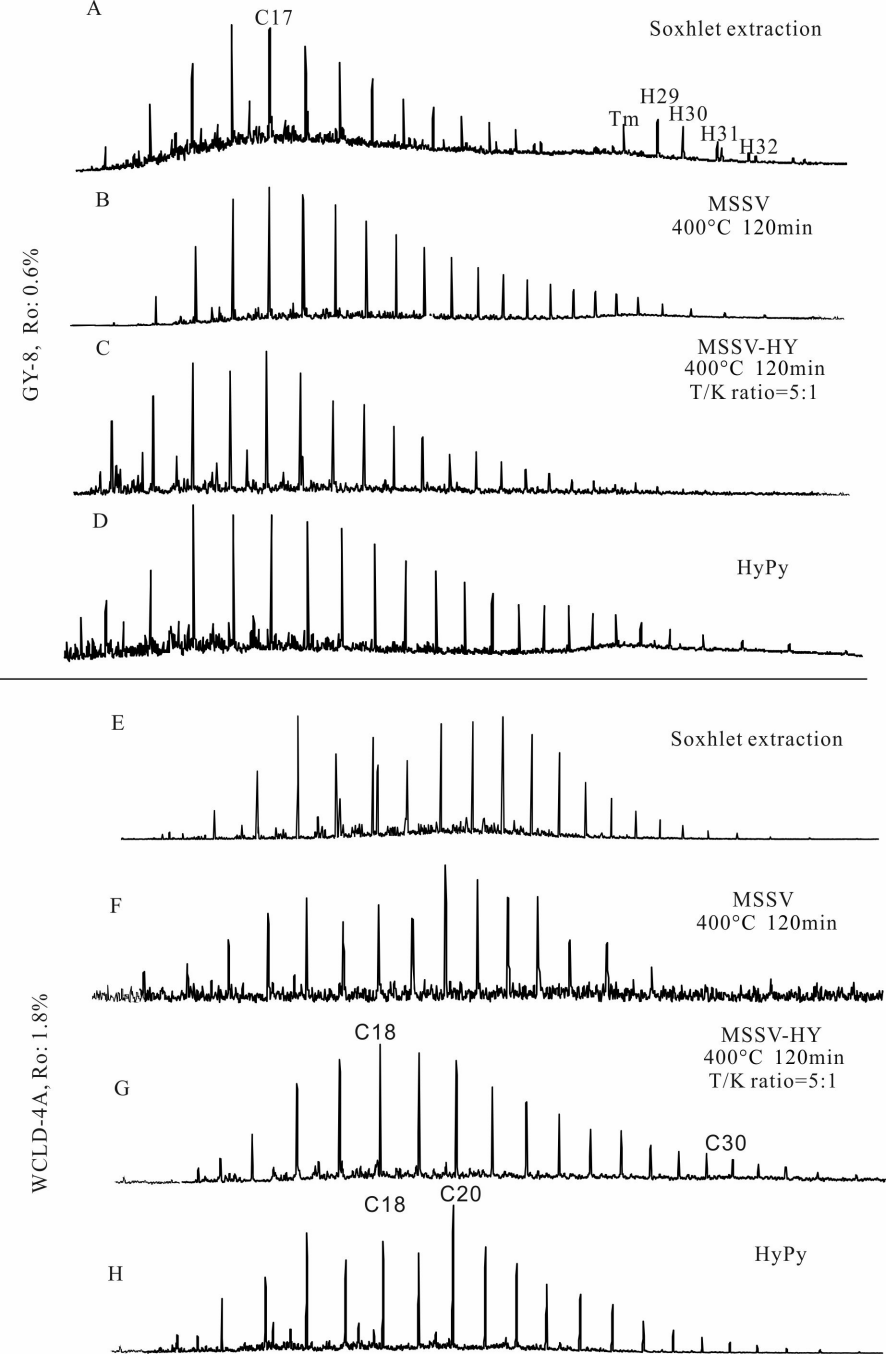
A
C17
Soxhlet extraction
H29
Tm
H30
H31
H32
B
MSSV
400°C 120min
C
MSSV-HY
400°C 120min
T/K ratio=5:1
D
HyPy
GY-8, Ro: 0.6%
E
Soxhlet extraction
F
MSSV
400°C 120min
C18
MSSV-HY
400°C 120min
T/K ratio=5:1
G
C30
C18
C20
H
HyPy
WCLD-4A, Ro: 1.8%

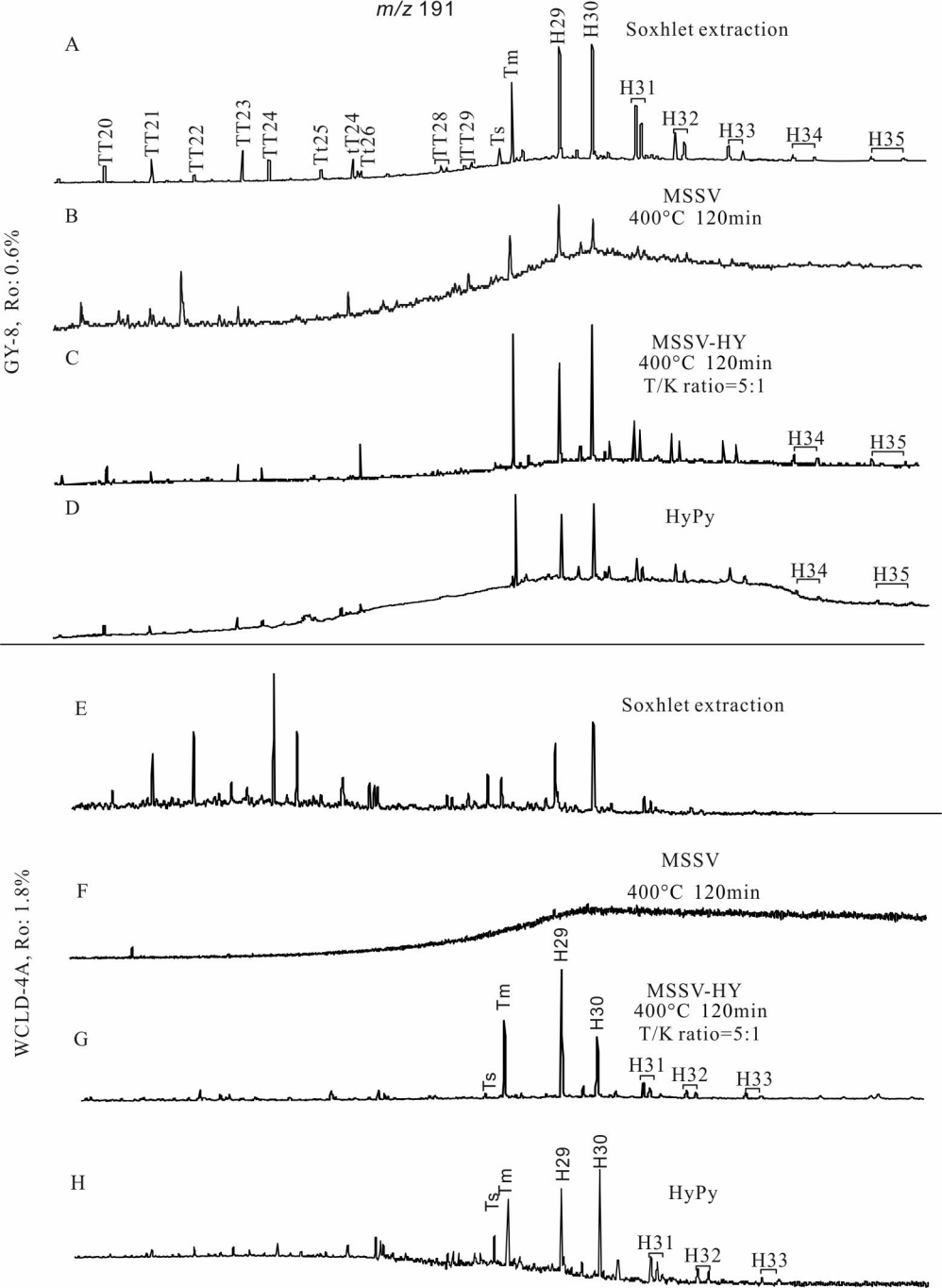
m/z 191
A
Soxhlet extraction
TT20
TT21
TT22
TT23
TT24
Tt25
tT24
Tt26
TT28
TT29
Ts
Tm
H29
H30
H31
H32
H33
H34
H35
B
MSSV
400°C 120min
C
MSSV-HY
400°C 120min
T/K ratio=5:1
D
HyPy
GY-8, Ro: 0.6%
E
Soxhlet extraction
F
MSSV
400°C 120min
G
MSSV-HY
400°C 120min
T/K ratio=5:1
H
HyPy
WCLD-4A, Ro: 1.8%

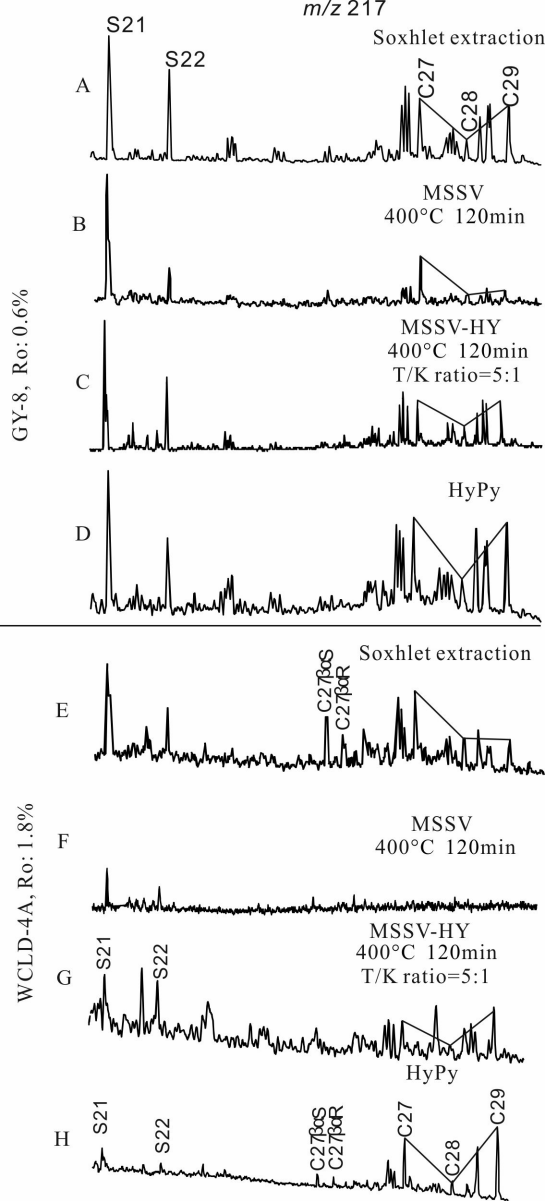
m/z 217
S21
S22
C27
C28
C29
A
Soxhlet extraction
B
MSSV
400°C 120min
C
MSSV-HY
400°C 120min
T/K ratio=5:1
D
HyPy
GY-8, Ro: 0.6%
E
C27βαS
C27βαR
Soxhlet extraction
F
MSSV
400°C 120min
G
S21
S22
MSSV-HY
400°C 120min
T/K ratio=5:1
HyPy
H
S21
S22
C27βαS
C27βαR
C27
C28
C29
WCLD-4A, Ro: 1.8%